## Artificial topological insulator realized in a two-terminal Josephson junction with Rashba spin-orbit interaction

Luka Medic ,\* Anton Ramšak , and Tomaž Rejec Jožef Stefan Institute, Jamova 39, SI-1000 Ljubljana, Slovenia and Faculty of Mathematics and Physics, University of Ljubljana, Jadranska 19, SI-1000 Ljubljana, Slovenia

(Received 21 August 2024; accepted 29 January 2025; published 14 February 2025)

We study a two-terminal Josephson junction with conventional superconductors and a normal region with a Rashba spin-orbit interaction, characterized by two Aharonov-Casher (AC) fluxes. When the superconducting phase difference equals  $\pi$ , the Andreev subgap spectrum may host zero-energy Weyl singularities associated with a vanishing normal-state reflection eigenvalue. With one of the AC fluxes playing the role of a quasimomentum, the junction can be viewed as an artificial one-dimensional chiral topological insulator. Its topological phase can be tuned by crossing a Weyl singularity by means of varying the remaining AC flux. By associating an additional component of the quasimomentum with the superconducting phase difference, an artificial Chern insulator is realized.

DOI: 10.1103/PhysRevResearch.7.013166

#### I. INTRODUCTION

The exploration of topology in condensed matter physics has flourished in recent decades [1-3]. Notably, Riwar et al. [4] introduced a novel class of topological systems by demonstrating that combining topologically trivial superconducting leads to form a multiterminal Josephson junction may result in a topologically nontrivial system, an artificial topological material, where independent superconducting phase differences act as quasimomenta in a synthetic Brillouin zone (BZ). Central to their proposal were superconductingphase-dependent Andreev bound states (ABSs), which could undergo a topological phase transition, leading to a change in the topological invariant, the Chern number. Consequently, the system exhibits quantization of the transconductance, which represents the current response in one terminal to the voltage applied to another. Eriksson et al. [5] numerically analyzed the same system and confirmed the quantization of the transconductance. Research was also done on threeterminal junctions in the presence of magnetic flux through the normal region [6,7]. In these systems, the Aharonov-Bohm phase associated with the magnetic flux serves as the control parameter. Although experimental studies on multiterminal Josephson junctions have been conducted [8–13], a demonstration of the quantization of the transconductance is still missing.

In this paper, similar to Ref. [6], we introduce another control phase. Instead of the magnetic flux and the associated Aharonov-Bohm phase, we study systems exhibiting

Published by the American Physical Society under the terms of the Creative Commons Attribution 4.0 International license. Further distribution of this work must maintain attribution to the author(s) and the published article's title, journal citation, and DOI.

the spin-dependent Aharonov-Casher (AC) effect in the presence of the electric field [14–19]. In quasi-one-dimensional quantum wires, the AC phase can be induced by the Rashba spin-orbit coupling [20-23], where electrons with opposite spins acquire opposite phases [24–26]. For an InGaAs-based two-dimensional electron gas, the Rashba coupling, which can be controlled by a gate voltage, typically takes values in the range of  $(0.5-2.0) \times 10^{-11}$  eV m [27-29]. In Rashba-gatecontrolled rings [28-31], this corresponds to values of the AC flux between  $0.3\pi$  and  $3\pi$ .

Studies on the effects of spin-orbit interaction in multiterminal Josephson junctions have already been conducted [32,33]. These investigations examined the ABS spectrum, including the impact of spin-orbit interaction on Weyl nodes and superconducting gap edge touchings. However, the consideration of spin-orbit phenomena as a possibility for the quasimomentum of a synthetic BZ has not been explored in these works.

Here, we present a theoretical analysis focused on the exploration of low-dimensional, topologically nontrivial artificial materials utilizing the Rashba interaction within the normal region. The minimal model consists of a two-terminal Josephson junction with a normal region composed of two rings, as depicted in Fig. 1, each permeated by an AC flux. Our investigation concludes that both the winding number and the Chern number can be identified in this system. For the Chern number, the system's synthetic BZ consists of an AC flux and the superconducting phase difference, whereas for the winding number, the superconducting phase difference is fixed to  $\pi$ .

The paper is organized to first analyze the symmetries of a general multiterminal system with multiple AC fluxes in the normal region and obtain the topological classification for this family of systems. Subsequently, we restrict ourselves to the analysis of systems with only two leads and two AC fluxes. The winding number is computed, and with the help of the low-energy Hamiltonian at the Weyl node, its connection

<sup>\*</sup>Contact author: luka.medic@ijs.si

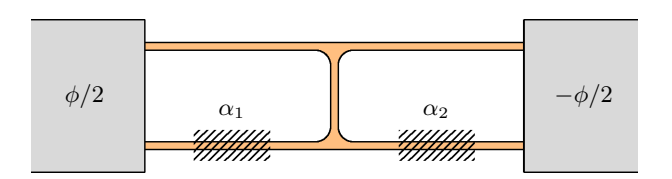


FIG. 1. SNS Josephson junction with a superconducting phase difference  $\phi$  and a normal region (orange) consisting of interconnected quantum wires, forming two rings (genus 2). Each ring can be assigned an independent AC flux ( $\alpha_{1,2}$ ), controllable via Rashba coupling using gate electrodes (hatched).

to the Chern number is established. Utilizing the system's symmetries, we conclude that for each spin sector, Weyl nodes come in quartets with pairs of opposite topological charges.

#### II. SYMMETRIES

We consider a general case of a multiterminal Josephson junction in the presence of AC fluxes in the normal region. The parameters of our model encompass a vector  $\vec{\phi}$  containing the independent superconducting phase differences, and a vector  $\vec{\alpha}$  describing the AC fluxes through the normal region. Specifically, there is one AC flux for each ring (refer to Fig. 1).

We begin with the electron Hamiltonian, which describes the system in its normal state and has the following structure [28,29]:

$$H(\vec{\alpha}) = \begin{bmatrix} H_{\uparrow}(\vec{\alpha}) & 0 \\ 0 & H_{\downarrow}(\vec{\alpha}) \end{bmatrix}. \tag{1}$$

Since electrons with opposite spins acquire opposite AC phases, the nonzero blocks satisfy the relations  $H_{\downarrow}(\vec{\alpha}) = H_{\uparrow}(-\vec{\alpha}) = H_{\uparrow}(\vec{\alpha})^*$ . Consequently, H exhibits symmetry under conjugation and time-reversal symmetry (TRS),

$$H(\vec{\alpha})^* = H(-\vec{\alpha}), \tag{2a}$$

$$TH(\vec{\alpha})T^{-1} = H(\vec{\alpha}), \tag{2b}$$

where  $T = i\sigma_y \mathcal{K}$ ; here,  $\sigma_y$  is the Pauli matrix operating on the spin degree of freedom, and  $\mathcal{K}$  is the conjugation operator.

This allows us to represent the Bogoliubov-de Gennes (BdG) Hamiltonian, which incorporates the description of superconductivity, as

$$H_{\text{BdG}}(\vec{\phi}, \vec{\alpha}) = \begin{bmatrix} H(\vec{\alpha}) & \Delta(\vec{\phi}) \\ \Delta(\vec{\phi})^{\dagger} & -TH(\vec{\alpha})T^{-1} \end{bmatrix}, \tag{3}$$

where  $\Delta(\vec{\phi})$  is a diagonal matrix for the s-wave pairing. In this form of the BdG Hamiltonian, the intrinsic particle-hole symmetry (PHS) is expressed as

$$\tau_{y}\sigma_{y}H_{\mathrm{BdG}}^{*}(\vec{\alpha},\vec{\phi})\sigma_{y}\tau_{y} = -H_{\mathrm{BdG}}(\vec{\alpha},\vec{\phi}),\tag{4}$$

where  $\tau_y$  is the Pauli matrix acting in the Nambu space. Additionally, from Eq. (2) and the relations  $T\Delta(\vec{\phi})T^{-1} = \Delta(\vec{\phi})^* = \Delta(-\vec{\phi})$ , it follows that the BdG Hamiltonian also exhibits symmetry under conjugation and TRS:

$$H_{\text{BdG}}^*(\vec{\alpha}, \vec{\phi}) = H_{\text{BdG}}(-\vec{\alpha}, -\vec{\phi}),$$
 (5a)

$$\sigma_{\mathbf{v}} H_{\mathrm{BdG}}^*(\vec{\alpha}, \vec{\phi}) \sigma_{\mathbf{v}} = H_{\mathrm{BdG}}(\vec{\alpha}, -\vec{\phi}).$$
 (5b)

TABLE I. Classification table for the case where the control parameter is a superconducting phase difference, resulting in the exclusive presence of PHS [Eq. (6a)] within each spin sector. Bott periodicity implies a periodic structure in  $d_{\phi}$  and  $d_{\alpha}$  with a period of 8.

	$d_{\phi}$							
$d_{\alpha}$	0	1	2	3	4	5	6	7
0	0	0	$\mathbb{Z}$	$\mathbb{Z}_2$	$\mathbb{Z}_2$	0	$2\mathbb{Z}$	0
1	0	0	0	$\mathbb{Z}$	$\mathbb{Z}_2$	$\mathbb{Z}_2$	0	$2\mathbb{Z}$
2	$2\mathbb{Z}$	0	0	0	$\mathbb{Z}$	$\mathbb{Z}_2$	$\mathbb{Z}_2$	0
3	0	$2\mathbb{Z}$	0	0	0	$\mathbb{Z}$	$\mathbb{Z}_2$	$\mathbb{Z}_2$
4	$\mathbb{Z}_2$	0	$2\mathbb{Z}$	0	0	0	$\mathbb{Z}$	$\mathbb{Z}_2$
5	$\mathbb{Z}_2$	$\mathbb{Z}_2$	0	$2\mathbb{Z}$	0	0	0	$\mathbb{Z}$
6	$\mathbb{Z}$	$\mathbb{Z}_2$	$\mathbb{Z}_2$	0	$2\mathbb{Z}$	0	0	0
7	0	$\mathbb{Z}$	$\mathbb{Z}_2$	$\mathbb{Z}_2$	0	$2\mathbb{Z}$	0	0

The BdG Hamiltonian is symmetric under  $\sigma_z$ , i.e.,  $\sigma_z H_{\rm BdG}(\vec{\alpha}, \vec{\phi}) \sigma_z = H_{\rm BdG}(\vec{\alpha}, \vec{\phi})$ , so the Hilbert space splits into two spin sectors. Hence, our focus lies on the classification within each sector. Combining Eqs. (4) and (5), we obtain two symmetries that do not mix the spin sectors,

$$\tau_{\nu} H_{\text{BdG}}^*(\vec{\alpha}, \vec{\phi}) \tau_{\nu} = -H_{\text{BdG}}(-\vec{\alpha}, \vec{\phi}), \tag{6a}$$

$$\tau_{\mathbf{v}} H_{\mathrm{BdG}}(\vec{\alpha}, \vec{\phi}) \tau_{\mathbf{v}} = -H_{\mathrm{BdG}}(\vec{\alpha}, -\vec{\phi}), \tag{6b}$$

which can be regarded as PHS and chiral symmetry (CS) within each sector. Note that, as a combination of TRS and the intrinsic PHS, chiral symmetry is generally preserved even in more complex Rashba interaction models.

### III. TOPOLOGICAL CLASSIFICATION

To transition a system between different topological phases, it is necessary to introduce at least one control parameter. Here, we focus on two scenarios: using either a single superconducting phase difference or a single AC flux as the control parameter. Selecting a superconducting phase difference as the control parameter breaks the CS described in Eq. (6b) while preserving the PHS described in Eq. (6a). Conversely, choosing an AC flux as the control parameter breaks the PHS while leaving the CS unaffected. Referring to Ref. [34], we have constructed topological classification tables for both scenarios (see Tables I and II); for specifics, refer to Supplemental Material (SM) S1 [35]. In the tables,  $d_{\phi}$  and  $d_{\alpha}$  denote the dimensionalities of phases composing the

TABLE II. Classification table for the case where an AC flux is used as the control parameter, maintaining CS [Eq. (6b)] within each spin sector.

	$d_{\phi}$			
$d_{lpha}$	Even	Odd		
Even Odd	0 Z	$egin{pmatrix} 0 \ \mathbb{Z} \oplus \mathbb{Z} \ \end{pmatrix}$		
Odd	<u> </u>	∠ ⊕ ∠		

synthetic BZ, culminating in its total dimensionality  $d_{\rm BZ} = d_{\phi} + d_{\alpha}$ .

In Table I, the case  $[d_{\phi}=2,d_{\alpha}=0]$ , having a topological invariant  $\mathbb{Z}$ , corresponds to the system with a nontrivial Chern number investigated in Ref. [4]. Specifically, the minimal model constitutes a four-terminal Josephson junction featuring three independent superconducting phases. Among these phases, two contribute to defining the synthetic BZ, while the remaining one functions as the control phase.

From here on, we restrict our analysis to systems with two superconducting leads only. In Table I, another consideration for identifying topologically nontrivial phases in low-dimensional systems is the option  $[d_{\phi}=0,d_{\alpha}=2]$ . In this case, the control parameter is the superconducting phase difference  $\phi$ . Yet, as we will delve into in the subsequent sections, all the topological charges are situated at  $\phi=\pi$  with a total charge of 0. Consequently, the behavior manifests as trivial.

Selecting one of the AC fluxes as the control parameter, Table II reveals that the lowest-dimensional nontrivial cases are  $\mathbb{Z}$  and  $\mathbb{Z} \oplus \mathbb{Z}$  for  $[d_{\phi} = 0, d_{\alpha} = 1]$  and  $[d_{\phi} = 1, d_{\alpha} = 1]$ , respectively. Here,  $\mathbb{Z}$  represents the winding number, while  $\mathbb{Z} \oplus \mathbb{Z}$  corresponds to the Chern number and the mirror winding number [34,36,37]. In the former case, the presence of CS requires the superconducting phase difference to be either 0 or  $\pi$ . Additionally, to allow for gap closures and enable topological phase transitions, we set  $\phi = \pi$ . Conversely, in the latter case, this constraint is lifted and  $\phi$  is treated as a quasimomentum. For the remainder of the paper, our focus will be on these two cases, i.e., a two-terminal Josephson junction featuring two AC fluxes in the normal region.

#### IV. EFFECTIVE HAMILTONIAN

We begin with the expression determining the Andreev bound states with energy E ( $|E| < |\Delta|$ ) within the sector corresponding to electrons (holes) with spin  $\uparrow$  ( $\downarrow$ ) [33,38,39],

$$\begin{bmatrix} 0 & S_{\uparrow}(\vec{\alpha}) e^{i\hat{\phi}} \\ S_{\downarrow}^{*}(\vec{\alpha}) e^{-i\hat{\phi}} & 0 \end{bmatrix} \psi = e^{i\chi} \psi, \tag{7}$$

where  $\chi \equiv \arccos(E/|\Delta|)$ , with leads having the same gap  $|\Delta|$ . The components of  $\psi = [\psi_e, \psi_h]^T$  are the amplitudes of the outgoing waves for electrons and holes. The matrix  $\hat{\phi} = \operatorname{diag}(\phi/2, -\phi/2) \otimes \mathbb{I}_N$  is diagonal, where  $\phi \in [0, 2\pi)$ denotes the superconducting phase difference, and  $\mathbb{I}_N$  signifies the identity matrix with dimension N, indicating the number of modes in each lead. (We assume for simplicity that the number of modes in both leads is the same.)  $S_{\uparrow}$  ( $S_{\downarrow}^*$ ) represents the normal-state scattering matrix for electrons (holes) with spin  $\uparrow (\downarrow)$ ; it is worth noting that  $S_{\downarrow}(\vec{\alpha}) = S_{\uparrow}^{T}(\vec{\alpha})$ . In the following, we will focus on the short junction limit, described by an energy-independent scattering matrix, and use the abbreviation  $S = S_{\uparrow}(\vec{\alpha})$ . A longer scattering region, characterized by an energy-dependent matrix S(E), would lead to additional ABSs at finite energy. Nevertheless, the existence of Weyl nodes and their topological properties at zero energy depend solely on S(0).

From Eq. (7), the equation for the electron part [40] can be obtained [4,38],

$$A\psi_e = e^{2i\chi}\psi_e,\tag{8}$$

where  $A = Se^{i\hat{\phi}}S^{\dagger}e^{-i\hat{\phi}}$  is unitary. Similar to the Joukowsky transform [41], we decompose  $A = A_1 + iA_2$  into its Hermitian and anti-Hermitian component, where  $A_1 = \frac{1}{2}(A + A^{\dagger})$  and  $A_2 = \frac{1}{2i}(A - A^{\dagger})$  are both Hermitian matrices. Separating the two parts of Eq. (8) yields a system of equations,

$$\left(\frac{\mathbb{I}_N - A_1}{2}\right)^{1/2} \psi_e = \sin \chi \ \psi_e, \tag{9a}$$

$$A_2 \psi_e = 2 \cos \chi \sin \chi \, \psi_e, \tag{9b}$$

where

$$\mathbb{I}_N - A_1 = 2\sin^2\frac{\phi}{2} \begin{bmatrix} t't'^{\dagger} & 0\\ 0 & tt^{\dagger} \end{bmatrix}, \tag{10a}$$

$$A_2 = 2\sin\frac{\phi}{2} \begin{bmatrix} -t't'^{\dagger}\cos\frac{\phi}{2} & rt^{\dagger}e^{i\frac{\phi}{2}} \\ tr^{\dagger}e^{-i\frac{\phi}{2}} & tt^{\dagger}\cos\frac{\phi}{2} \end{bmatrix}. \quad (10b)$$

Here, r(r') and t(t') are  $N \times N$  reflection and transmission matrices at the left (right) lead, respectively, and  $(\mathbb{I}_N - A_1)$  is positive semidefinite. In Eq. (9a), we took into account the constraint  $\mathrm{Im}(e^{i\chi}) \geqslant 0$  [38], i.e.,  $\chi \in [0,\pi]$ . Assuming that  $(\mathbb{I}_N - A_1)$  and  $A_2$  are nonsingular (requiring  $\phi \neq 0$ ), we can combine Eqs. (9a) and (9b) to derive the effective (electron) Hamiltonian acting in the ABS subspace,  $H_e \psi_e = E \psi_e$ , given by

$$H_e = |\Delta| \begin{bmatrix} -(t't'^{\dagger})^{1/2} \cos \frac{\phi}{2} & rt^{\dagger}(tt^{\dagger})^{-1/2} e^{i\phi/2} \\ (tt^{\dagger})^{-1/2} tr^{\dagger} e^{-i\phi/2} & (tt^{\dagger})^{1/2} \cos \frac{\phi}{2} \end{bmatrix}. \tag{11}$$

The eigenvalues of  $H_e$  come in pairs  $E_n^{\pm} = \pm |\Delta| \sqrt{1 - T_n \sin^2(\phi/2)}$ , where  $T_n$  are eigenvalues of  $tt^{\dagger}$  [38]. Thus, the gap closes when  $\phi = \pi$  and  $T_n = 1$ . In the limit  $\phi \to 0$ , ABSs approach the continuum at  $\pm |\Delta|$ .

#### V. CHIRAL SYMMETRY

The chiral symmetry [Eq. (6b)] implies that eigenfunctions appear in pairs with opposite energies, satisfying  $\Psi(\vec{\alpha}, -\vec{\phi}) = i\tau_y \Psi(\vec{\alpha}, \vec{\phi})$ . This results in CS effectively swapping the roles of incoming and outgoing waves. Additionally, incoming waves are related to outgoing waves through Andreev reflection [38]. Consequently, under chiral symmetry, the components of outgoing waves  $(\psi_e, \psi_h)$  transform to  $(e^{-i\hat{\phi}-i\chi}\psi_e, -e^{i\hat{\phi}-i\chi}\psi_h)$ .

Focusing on the electron component, the effective Hamiltonian from the previous section satisfies  $e^{i\hat{\phi}}H_e(\vec{\alpha},2\pi-\phi)e^{-i\hat{\phi}}=-H_e(\vec{\alpha},\phi).$  For  $\phi=\pi$ , this reduces to  $\Gamma_{\pi}H_e\Gamma_{\pi}^{\dagger}=-H_e$ , where  $\Gamma_{\pi}=\nu_z\otimes\mathbb{I}_N$  and  $\nu_z$  is the Pauli matrix acting in the space of left- and right-outgoing waves. This is unsurprising, as  $H_e$  becomes block off-diagonal at  $\phi=\pi$ .

# VI. TOPOLOGICAL INVARIANTS AND THE LOW-ENERGY HAMILTONIAN

We proceed by determining the topological invariant at  $\phi = \pi$ . From the topological classification, we already know

that the appropriate invariant is the winding number [34,42]. However, because the winding number is gauge dependent, we will consider the differences between winding numbers at different values of the control AC flux. These differences correspond to contractible (i.e., null-homotopic) loops in the space of AC fluxes. For such loops, we derive

$$W_{\pi} = \frac{1}{2\pi i} \oint_{\mathcal{C}_{\pi}} d\log\left(\det h\right) = \frac{1}{2\pi i} \oint_{\mathcal{C}_{\pi}} d\log\left(\det r\right), \quad (12)$$

where  $\mathcal{C}_{\alpha}$  is an arbitrary contractible loop, and  $h=irt^{\dagger}(tt^{\dagger})^{-1/2}$  is the off-diagonal block of  $H_e$ . In the last step, we assumed that  $\mathcal{C}_{\alpha}$  does not cross or enclose any gap edge touchings. Consequently, only the reflection matrix r contributes to  $W_{\pi}$ .

Next, let us focus on the low-energy limit, particularly on the band touching at a Weyl node located at  $\vec{x}_W = [\alpha_{1W}, \alpha_{2W}, \pi]^T$ . Denoting the two chiral states at the Weyl node with positive and negative chirality as  $|a_e^+\rangle$  and  $|a_e^-\rangle$ , respectively (where  $\nu_z |a_e^\pm\rangle = \pm |a_e^\pm\rangle$ ), we can express the low-energy Hamiltonian as (details in SM S2 [35])

$$H_W = \delta \vec{x} \cdot M_3 \vec{\Sigma}. \tag{13}$$

Here,  $\delta \vec{x} = [\delta \alpha_1, \delta \alpha_2, \delta \phi]^T$  represents the displacement from the Weyl node,  $\vec{\Sigma}$  is a vector of Pauli matrices acting in the space of chiral states  $|a_e^{\pm}\rangle$ , and

$$M_{3} = \begin{bmatrix} M_{2} & 0 \\ 0 & 0 \\ \hline 0 & 0 & \frac{1}{2} \end{bmatrix},$$

$$M_{2} = \begin{bmatrix} \partial_{\alpha_{1}} \operatorname{Re}(\zeta) & -\partial_{\alpha_{1}} \operatorname{Im}(\zeta) \\ \partial_{\alpha_{2}} \operatorname{Re}(\zeta) & -\partial_{\alpha_{2}} \operatorname{Im}(\zeta) \end{bmatrix}_{\vec{x} = \vec{x}_{W}}, \tag{14}$$

where  $\zeta(\vec{x}) = \langle a_e^+ | H_e(\vec{x}) | a_e^- \rangle$ , and  $M_2$  is evaluated at the Weyl node. Thus, the low-energy dispersion at the Weyl node is conical, given by  $E^\pm = \pm \sqrt{|\delta \vec{\alpha} \cdot \nabla_{\vec{\alpha}} \zeta|^2 + (\delta \phi/2)^2}$ .

From Eq. (14), topological charges associated with winding and Chern numbers can be obtained as  $W_W = \text{sgn}[\det(M_2)]$  and  $C_W = \text{sgn}[\det(M_3)]$ , respectively. It is clear that the two charges are equivalent, and we henceforth denote them as  $q_W$ .

Following the topological classification of the BdG Hamiltonian presented in Table II, the remaining invariant is the mirror winding number, defined as [36]

$$W_{MZ} = \operatorname{sgn}[W_0 - W_{\pi}](|W_0| - |W_{\pi}|), \tag{15}$$

where  $W_0$  is the winding number evaluated in the plane  $\phi = 0$ . Although the winding number is well defined for the entire BdG Hamiltonian, our approach involving scattering matrices and ABSs, which merge with the continuum, does not permit us to obtain  $W_0$  in our present formulation. We leave the calculation of the mirror winding number of the BdG Hamiltonian for further study.

Applying conjugation symmetry, Eq. (5a), at the conjugation-invariant phase  $\phi = \pi$  [43], leads us to the conclusion that Weyl nodes come in pairs at  $\pm \vec{x}_W$  with equal topological charges,  $q_W(\vec{x}_W) = q_W(-\vec{x}_W)$ . Given this equivalence of topological charges and considering the Nielsen-Ninomiya theorem, which necessitates total charge cancellation [44–46], we infer the existence of quartets of

Weyl nodes within each spin sector. Each quartet comprises two Weyl nodes with positive topological charge and two with negative topological charge.

Considering both sectors, the TRS [Eq. (5b)] implies that  $q_W^{\downarrow}(\vec{x}_W) = q_W^{\uparrow}(-\vec{x}_W) = q_W^{\uparrow}(\vec{x}_W)$ , resulting in both sectors having identical topological charges at  $\vec{x}_W$ . Consequently, eigenstates at the Weyl nodes are topologically protected and can be gapped only by the annihilation of opposite charges. The total charge, combining charges for both sectors, amounts to twice the topological charge for each individual sector.

#### VII. DISCUSSION

To summarize, we provided a topological classification of multiterminal Josephson junctions with AC fluxes in the normal region. In contrast to previous proposals for realizing Josephson junctions as topological matter [4,6,7], we showed that topologically nontrivial regimes can arise even in Josephson junctions with just two terminals. Specifically, for two-terminal Josephson junctions with the superconducting phase difference equal to  $\pi$ , we demonstrated that when no gap edge touchings are enclosed by  $\mathcal{C}_{\alpha}$ , the computation of winding number differences simplifies to the topological properties of the reflection matrix r. We confirmed that the dispersion near zero-energy singularities is conical, identifying these singularities as Weyl nodes. Additionally, we established the equivalence between the topological charges associated with the winding number and the Chern number. Finally, we showed that the Weyl nodes of the two spin sectors coincide and carry the same topological charges.

In our approach, we derived ABS spectra using scattering matrices. However, by neglecting the energy dependence of these matrices, we encountered ABS spectra with gap edge touchings. Incorporating energy dependence in the scattering matrix could introduce finite level repulsion between the highest ABS and the continuum, thereby restoring the adiabaticity of the ABSs, as discussed in Ref. [4]. Furthermore, as highlighted in the main text, another limitation of this scattering formalism and ABS-based approach is its inability to compute the mirror winding number of the BdG Hamiltonian. To address this, analytical generalizations similar to those proposed in Ref. [47] may be required. Further exploration of these ideas is a direction for future theoretical research.

Another challenge stems from the constrained variation range of the AC flux. To handle this limitation, a protocol should be devised that does not require quasimomentum variations exceeding  $2\pi$ , unlike the protocol presented in Ref. [4]. The proposed protocol should identify a quantized physical observable related to either the winding number or the Chern number (or their associated topological charges). It is important to note that, unlike superconducting phases, which are associated with electric currents, AC fluxes are related to spin currents. Further research along these lines is detailed in a separate publication [48].

While we acknowledge that experimentally realizing the proposed systems remains challenging, we hope our results will inspire efforts toward the development of such devices.

#### ACKNOWLEDGMENTS

We appreciate valuable discussions with Y. V. Nazarov and R. Žitko. The authors acknowledge support from the Slovenian Research and Innovation Agency (ARIS) under Contract No. P1-0044; A.R. was also supported by Grant No. J2-2514.

- [1] C.-K. Chiu, J. C. Y. Teo, A. P. Schnyder, and S. Ryu, Classification of topological quantum matter with symmetries, Rev. Mod. Phys. 88, 035005 (2016).
- [2] M. Z. Hasan and C. L. Kane, Colloquium: Topological insulators, Rev. Mod. Phys. **82**, 3045 (2010).
- [3] X.-L. Qi and S.-C. Zhang, Topological insulators and superconductors, Rev. Mod. Phys. **83**, 1057 (2011).
- [4] R.-P. Riwar, M. Houzet, J. S. Meyer, and Y. V. Nazarov, Multi-terminal Josephson junctions as topological matter, Nat. Commun. 7, 11167 (2016).
- [5] E. Eriksson, R.-P. Riwar, M. Houzet, J. S. Meyer, and Y. V. Nazarov, Topological transconductance quantization in a four-terminal Josephson junction, Phys. Rev. B 95, 075417 (2017).
- [6] J. S. Meyer and M. Houzet, Nontrivial Chern numbers in threeterminal Josephson junctions, Phys. Rev. Lett. 119, 136807 (2017).
- [7] H.-Y. Xie, M. G. Vavilov, and A. Levchenko, Topological Andreev bands in three-terminal Josephson junctions, Phys. Rev. B 96, 161406(R) (2017).
- [8] A. H. Pfeffer, J. E. Duvauchelle, H. Courtois, R. Mélin, D. Feinberg, and F. Lefloch, Subgap structure in the conductance of a three-terminal Josephson junction, Phys. Rev. B 90, 075401 (2014).
- [9] E. Strambini, S. D'Ambrosio, F. Vischi, F. S. Bergeret, Yu. V. Nazarov, and F. Giazotto, The  $\omega$ -SQUIPT as a tool to phase-engineer Josephson topological materials, Nat. Nanotechnol. **11**, 1055 (2016).
- [10] Y. Cohen, Y. Ronen, J.-H. Kang, M. Heiblum, D. Feinberg, R. Mélin, and H. Shtrikman, Nonlocal supercurrent of quartets in a three-terminal Josephson junction, Proc. Natl. Acad. Sci. USA 115, 6991 (2018).
- [11] A. W. Draelos, M.-T. Wei, A. Seredinski, H. Li, Y. Mehta, K. Watanabe, T. Taniguchi, I. V. Borzenets, F. Amet, and G. Finkelstein, Supercurrent flow in multiterminal graphene Josephson junctions, Nano Lett. 19, 1039 (2019).
- [12] G. V. Graziano, J. S. Lee, M. Pendharkar, C. J. Palmstrøm, and V. S. Pribiag, Transport studies in a gate-tunable three-terminal Josephson junction, Phys. Rev. B 101, 054510 (2020).
- [13] N. Pankratova, H. Lee, R. Kuzmin, K. Wickramasinghe, W. Mayer, J. Yuan, M. G. Vavilov, J. Shabani, and V. E. Manucharyan, Multiterminal Josephson effect, Phys. Rev. X 10, 031051 (2020).
- [14] Y. Aharonov and A. Casher, Topological quantum effects for neutral particles, Phys. Rev. Lett. 53, 319 (1984).
- [15] A. Cimmino, G. I. Opat, A. G. Klein, H. Kaiser, S. A. Werner, M. Arif, and R. Clothier, Observation of the topological Aharonov-Casher phase shift by neutron interferometry, Phys. Rev. Lett. 63, 380 (1989).
- [16] H. Mathur and A. D. Stone, Quantum transport and the electronic Aharonov-Casher effect, Phys. Rev. Lett. 68, 2964 (1992).
- [17] M. König, A. Tschetschetkin, E. M. Hankiewicz, J. Sinova, V. Hock, V. Daumer, M. Schäfer, C. R. Becker, H. Buhmann, and

- L. W. Molenkamp, Direct observation of the Aharonov-Casher phase, Phys. Rev. Lett. **96**, 076804 (2006).
- [18] T. Bergsten, T. Kobayashi, Y. Sekine, and J. Nitta, Experimental demonstration of the time reversal Aharonov-Casher effect, Phys. Rev. Lett. 97, 196803 (2006).
- [19] X. Liu, M. F. Borunda, X.-J. Liu, and J. Sinova, Control of Josephson current by Aharonov-Casher phase in a Rashba ring, Phys. Rev. B 80, 174524 (2009).
- [20] E. I. Rashba, Symmetry of energy bands in crystals of wurtzite type II. Symmetry of bands with spin-orbit interaction included, Fiz. Tverd. Tela: Collected Papers 2, 62 (1959).
- [21] Yu. A. Bychkov and E. I. Rashba, Properties of a 2D electron gas with lifted spectral degeneracy, JETP Lett. 39, 78 (1984).
- [22] Yu. A. Bychkov and E. I. Rashba, Oscillatory effects and the magnetic susceptibility of carriers in inversion layers, J. Phys. C: Solid State Phys. 17, 6039 (1984).
- [23] G. Bihlmayer, O. Rader, and R. Winkler, Focus on the Rashba effect, New J. Phys. 17, 050202 (2015).
- [24] A. Manchon, H. C. Koo, J. Nitta, S. M. Frolov, and R. A. Duine, New perspectives for Rashba spin–orbit coupling, Nat. Mater. 14, 871 (2015).
- [25] D. Tomaszewski, P. Busz, R. López, R. Žitko, M. Lee, and J. Martinek, Aharonov-Bohm and Aharonov-Casher effects for local and nonlocal Cooper pairs, Phys. Rev. B 97, 214506 (2018).
- [26] D. Tomaszewski, P. Busz, R. López, R. Žitko, M. Lee, and J. Martinek, Aharonov-Bohm and Aharonov-Casher effects in a double quantum dot Josephson junction, Phys. Rev. B 98, 174504 (2018).
- [27] D. Grundler, Large Rashba splitting in InAs quantum wells due to electron wave function penetration into the barrier layers, Phys. Rev. Lett. 84, 6074 (2000).
- [28] R. Citro and F. Romeo, Pumping in a mesoscopic ring with Aharonov-Casher effect, Phys. Rev. B 73, 233304 (2006).
- [29] B. H. Wu and J. C. Cao, Analysis of spin pumping in asymmetric ring conductors with the Aharonov-Casher effect, Phys. Rev. B **75**, 113303 (2007).
- [30] F. Romeo, R. Citro, and M. Marinaro, Quantum pumping and rectification effects in Aharonov-Bohm-Casher ring-dot systems, Phys. Rev. B 78, 245309 (2008).
- [31] M. W.-Y. Tu, A. Aharony, W.-M. Zhang, and O. Entin-Wohlman, Real-time dynamics of spin-dependent transport through a double-quantum-dot Aharonov-Bohm interferometer with spin-orbit interaction, Phys. Rev. B 90, 165422 (2014).
- [32] B. Béri, J. H. Bardarson, and C. W. J. Beenakker, Splitting of Andreev levels in a Josephson junction by spin-orbit coupling, Phys. Rev. B 77, 045311 (2008).
- [33] T. Yokoyama and Y. V. Nazarov, Singularities in the Andreev spectrum of a multiterminal Josephson junction, Phys. Rev. B 92, 155437 (2015).
- [34] K. Shiozaki and M. Sato, Topology of crystalline insulators and superconductors, Phys. Rev. B 90, 165114 (2014).
- [35] See Supplemental Material at http://link.aps.org/supplemental/ 10.1103/PhysRevResearch.7.013166 for details on topologi-

- cal classification and an alternative approach utilizing the full Nambu space.
- [36] C.-K. Chiu, H. Yao, and S. Ryu, Classification of topological insulators and superconductors in the presence of reflection symmetry, Phys. Rev. B **88**, 075142 (2013).
- [37] F. Zhang and C. L. Kane, Anomalous topological pumps and fractional Josephson effects, Phys. Rev. B 90, 020501(R) (2014).
- [38] C. W. J. Beenakker, Universal limit of critical-current fluctuations in mesoscopic Josephson junctions, Phys. Rev. Lett. 67, 3836 (1991).
- [39] Y. V. Nazarov and Y. M. Blanter, *Quantum Transport: Introduction to Nanoscience* (Cambridge University Press, Cambridge, UK, 2009).
- [40] In Supplemental Material S2 [35], we present an alternative approach that considers both the electron and hole parts simultaneously. We demonstrate that the conclusions remain consistent with those obtained using the approach presented in this paper, which considered only the electron part when computing the effective Hamiltonian and the topological invariants. References [49,50] are included.
- [41] B. van Heck, S. Mi, and A. R. Akhmerov, Single fermion manipulation via superconducting phase differences in multiterminal Josephson junctions, Phys. Rev. B 90, 155450 (2014).
- [42] M. Maffei, A. Dauphin, F. Cardano, M. Lewenstein, and P. Massignan, Topological characterization of chiral models

- through their long time dynamics, New J. Phys. **20**, 013023 (2018).
- [43] Here, the conjugation symmetry, Eq. (5a), mimics TRS within each distinct sector, where  $\phi = \pi$  is analogous to time-reversal invariant momentum (TRIM).
- [44] H. B. Nielsen and M. Ninomiya, Absence of neutrinos on a lattice: (I). Proof by homotopy theory, Nucl. Phys. B 185, 20 (1981).
- [45] H. B. Nielsen and M. Ninomiya, Absence of neutrinos on a lattice: (II). Intuitive topological proof, Nucl. Phys. B 193, 173 (1981).
- [46] S. Murakami, Phase transition between the quantum spin Hall and insulator phases in 3D: Emergence of a topological gapless phase, New J. Phys. **9**, 356 (2007).
- [47] E. V. Repin, Y. Chen, and Y. V. Nazarov, Topological properties of multiterminal superconducting nanostructures: Effect of a continuous spectrum, Phys. Rev. B **99**, 165414 (2019).
- [48] L. Medic, A. Ramšak, and T. Rejec, A minimal model of an artificial topological material realized in a two-terminal Josephson junction threaded by Aharonov-Casher fluxes, arXiv:2412.09457.
- [49] Th. Martin and R. Landauer, Wave-packet approach to noise in multichannel mesoscopic systems, Phys. Rev. B 45, 1742 (1992).
- [50] C. W. J. Beenakker, Random-matrix theory of quantum transport, Rev. Mod. Phys. 69, 731 (1997).